Bandwidth considerations in modulated and transient photoconductivity measurements to determine localized state distributions

S. Reynolds[a] and C. Main
School of Science and Engineering, University of Abertay Dundee, Dundee DD1 1HG, United Kingdom

D. P. Webb
Department of Manufacturing Engineering, Loughborough University, Loughborough LE11 3TU, United Kingdom

S. Grabtchak
Department of Physics, University of Toronto, 60 St. George Street, Toronto, Ontario M5S 1A7, Canada

(Received 7 February 2000; accepted for publication 4 April 2000)

This work examines the influence of limited instrumental bandwidth on the accuracy of recovery of the density of localized states in semiconductors from transient and modulated photoconductivity data. Paradoxically, knowledge of the *short-time* transient photoresponse can be vital in the estimation, *via* a Fourier transform, of the density of *deep-lying* states. We demonstrate that retention of the natural response of a bandwidth limited system, although subject to distortion at short times, can lead to much improved accuracy in density of states determination than simple truncation of the short-time response. It is shown that this improvement arises simply from the integrating effect of a bandwidth limited system over short time intervals, which makes it possible to access and exploit information originating at times much shorter than the instrumentation rise time. These concepts are exemplified using computer simulated transient photoconductivity for several model systems including one which mimics the expected density of states in amorphous silicon. © *2000 American Institute of Physics.* [S0021-8979(00)07913-5]

I. INTRODUCTION

Transient photoconductivity (TPC) and modulated photoconductivity (MPC) are two closely related techniques which can yield information on the distribution of localized states $g(E)$ in amorphous semiconductor films.[1–6] TPC represents the impulse response of a semiconductor to a short flash of light, giving a time-dependent photocurrent $i(t)$, while MPC is the spectrum in the frequency domain, of the photocurrent response $I(\omega)$, to sinusoidally modulated optical excitation. In the context of a multitrapping model, each contains information on the trapping and release kinetics of excess charge carriers, in localized gap states, and hence on the density of states (DOS) function. Additionally, there is a formal mathematical relation between the impulse and frequency responses, provided the trapping system dynamics are linear. While this equivalence exists, it is nevertheless the case that the transitions characteristic of a given group of states are more clearly distinguished in the frequency domain than in the time domain. Thus at any instant in *time* in the TPC case, free electrons are interacting simultaneously with the whole range of localized states, making it difficult to discern the influence of any given group of states. In the MPC case,[4] however, at a given modulation *frequency* ω the amplitude and phase shift $\phi(\omega)$ of the free electron density and hence the photocurrent $I(\omega)$, with respect to the excitation, are dominated by a narrow band of states close to energy $E=kT\ln(\nu/\omega)$. Here, k is Boltzmann's constant, T is the temperature, and ν is the attempt-to-escape frequency.

A method of calculating $g(E)$ from MPC data was devised by Main,[7] based on earlier work by Hattori *et al.*[6] After some approximation, the expression

$$g(E)\approx \frac{1}{\nu\sigma kT}\,\omega\,\frac{d}{d\omega}\left(\frac{e\mu\mathcal{E}AG\cos(\phi(\omega))}{|I(\omega)|}\right) \tag{1}$$

is obtained, where ν is the electron thermal velocity, σ is the trap capture cross section, e is the electronic charge, μ is the electron mobility, $\mathcal{E}$ is the applied electric field strength, A is the conduction cross section, and G is the amplitude of the optical generation at frequency ω.

Experimentally, the frequency range available in MPC measurement using standard lock-in amplifier instrumentation is relatively limited, restricting the observable energy range available. Main *et al.*[1] showed that time sampled transient photoconductivity $i(t_k)$ may be transformed by numerical Fourier integral to give an approximate numerical result $I_n(\omega)$ for the frequency dependent photocurrent $I(\omega)$. Writing the Fourier transform as

$$I(\omega)=\int_0^\infty i(t)\exp(-j\omega t)dt, \tag{2}$$

then a simple numerical approximation is given by

[a]Author to whom corresspondence should be addressed; electronic mail: s.reynolds@tay.ac.uk

$$I_n(\omega)=\sum_{k=1}^{n}\tfrac{1}{2}[i(t_{k+1})\exp(-j\omega t_{k+1}) + i(t_k)\exp(-j\omega t_k]\Delta t_k \approx I(\omega), \quad (3)$$

where the interval $\Delta t_k = t_{k+1} - t_k$. Apart from the necessarily discrete nature of this approximation, it is evident that the experimental time interval cannot match that of the transform definition. Typically, the sample time range covered can be from a few nanoseconds to tens of seconds, so that in principle, a wider energy range may be accessed than is possible with MPC. However, a serious problem can arise[8] with the accuracy of the summation in Eq. (3) if short-time information is not accessible experimentally.

The shortest accessible time in TPC measurement is generally controlled by the combination of sample and preamplifier configurations. Usually there will be a related gain-bandwidth ''tradeoff'' so that to detect very low amplitude photocurrent transients, requiring a high system gain, one must accept a longer associated response time. Hence it has been normal practice to discard information from a time range shorter than the characteristic response time employed, or even up to ten times this value.[9]

We note here that the trapping time of free electrons into the ensemble of gap states in many amorphous semiconductors, e.g., amorphous silicon, may be as short as 10^{-12} s, much shorter than the typical instrumental response time, and hence the initial trapping processes cannot be directly accessed by such experiments.

In previous work,[8,10,11] we have examined the significance of ''missing'' short time data in the above calculation, with reference to the accuracy of recovery of the DOS. Essentially, we have shown that if the TPC is simply truncated, losing short time information, this can under certain conditions, result in severe distortion of the returned DOS over a wide range of energy. Initially, this may seem surprising, since it might be argued that the short time photocurrent should be influenced mostly by those states which achieve rapid thermal contact with the band, i.e., shallow traps. However, it is clear in the context of the Fourier integral of Eq. (2) above, that if the short-time photocurrent is high, and if there is a substantial fall in the current when trapping commences, then the contribution to the integral from the short-time component can be significant, even for low values of ω, which correspond to deep states in the DOS. Others[2,12] have also pointed out the vital importance of knowledge of the short-time current, to the validity of other DOS computation schemes.

In practice, the experimentally available time window would not normally allow this crucially important short time data to be accessed. To study the consequences of this, in an earlier work[11] we showed that it is possible to generate substantially the same long-time TPC decay using several different DOS distributions, for example: exponential, Gaussian, and flat, by an appropriate choice of parameters. Analysis of these decays using only the posttrapping current, which was close to a power-law form in all cases, results as expected in three almost indistinguishable exponential distributions. Only by extending the analysis to include the short-time ($t<10^{-11}$ s), pretrapping photocurrent could the different distributions be properly distinguished.

MPC measurement, on the other hand, does not suffer from errors caused by missing short-time data. The question thus arises—why should an MPC measurement made with a limited bandwidth provide a more accurate set of $I(\omega)$ data, albeit over its restricted range of validity—than the truncated and transformed TPC originating in a measurement made with an equal or wider bandwidth? In this article, we return to the question of the effect of limited instrumental bandwidth in the TPC experiment, but with a different treatment. Instead of representing the effect of the finite experimental time window by using a simple truncation of ideal computed TPC curves, we include the rather different, and perhaps more realistic, effect of a finite instrumental rise time, and outline ways of compensating for this, which retrieve the effect of the ''missing'' short-time information.

II. METHODS

The investigation required the computation of the ''ideal'' TPC, $i(t)$ vs t for selected $g(E)$ distributions, followed by either truncation or low-pass filtering of the original TPC with appropriate time constants, and then calculation of the DOS *via* Fourier transform of the processed data. The ''reconstituted'' DOS so obtained was then compared with the original.

To compute the TPC for a given $g(E)$, we first represent the continuous distribution of states with a fine ladder of closely spaced discrete levels, and then solve the resulting system of multitrapping rate equations, for free and trapped electron densities, with appropriate initial conditions for the excess electron density. The decay of the excess free electron density $\Delta n(t)$ from an initial value of $10^{15}\,\mathrm{cm}^{-3}$ is then extracted from the solution set, since it is proportional to the photocurrent $i(t)$. Efficient numerical solution schemes have been developed and are fully described in earlier publications.[13,14] The resulting simulated decay begins at times much shorter than the trapping time into the overall ensemble of traps, i.e., $t<10^{-12}$ s. To compare the two strategies, i.e., simple truncation versus bandwidth limitation, the ''exact,'' or full, decay was either truncated at a specified time t_i, or a numerical single pole low pass filter algorithm was applied, to replicate the bandwidth limited system response with characteristic time constant $\tau_i = t_i$. Finally the processed decays were subject to discrete Fourier integration starting in *each case* from an initial time t_i, and $g(E)$ was calculated using Eq. (1).

To illustrate clearly the operation of the proposed method we chose several representative model densities of states:

Flat:

$g(E)=g_0=10^{18}\ \mathrm{cm}^{-3}\,\mathrm{eV}^{-1}$; $\nu\sigma=10^{-6}\ \mathrm{cm}^3\,\mathrm{s}^{-1}$;

Exponential:

$g(E)=g_0\exp(-E/E_0)$; $g_0=10^{21}\ \mathrm{cm}^{-3}\,\mathrm{eV}^{-1}$;

$E_0=0.14$ eV; $\nu\sigma=10^{-8}\ \mathrm{cm}^3\,\mathrm{s}^{-1}$;

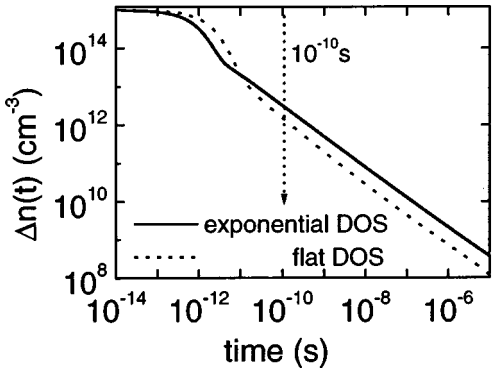

FIG. 1. Simulated decay of excess electron density $\Delta n(t)$ for the exponential and flat trap distributions. Parameters chosen to result in very similar power-law slopes in the posttrapping sections. Small differences in the short-time trapping regions contain information that distinguishes the two distributions.

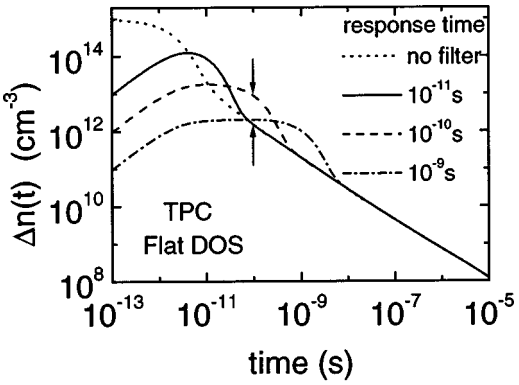

FIG. 2. Computed transient photocurrent for the flat distribution, showing the effects of bandwidth limitation with system time constants 10^{-11}, 10^{-10}, and 10^{-9} s. Integration and overshoot effects are evident. Arrows indicate the time 10^{-10} s from which the Fourier integrations started.

Amorphous silicon:[10]

$$g(E)=g_0\exp(-E/E_0)+g_d/\mathrm{sech}[(E-E_d)/E_1],$$

$$g_0=4\times10^{21}\ \mathrm{cm^{-3}eV^{-1}};\quad g_d=10^{17}\ \mathrm{cm^{-3}eV^{-1}};$$

$$E_0=0.03\ \mathrm{eV};\quad E_d=0.6\ \mathrm{eV};\quad E_1=0.06\ \mathrm{eV};$$

$$\nu\sigma=10^{-8}\ \mathrm{s^{-1}}.$$

The flat and exponential distributions are the same as used by Grabtchak *et al.*[11] and have parameters chosen to give closely similar trapping times and posttrapping decay slopes. The simplified model DOS for amorphous silicon was reported by Main *et al.*,[10] and contains a defect ''bump'' centered at a depth of 0.60 eV. It is well known that the TPC in *a*-Si:H exhibits a steep fall at about 10^{-7} s related to trapping into the deep defects. In this case, we wish to examine the consequences of missing the pre-''deep-trapping'' part of the TPC prior to 10^{-7} s rather than the initial pretrapping portion prior to 10^{-12} s.

III. RESULTS AND DISCUSSION

A. Exponential and flat distributions

In Fig. 1 we show the simulated TPC in the form of the excess electron decay, on log–log axes for the exponential and flat distributions. It is evident, as we have arranged, that the decays are very similar over the time window employed. The posttrapping sections have nearly identical power-law slopes. The trapping features are also similar, with apparently only minor differences in the trapping regions of the traces. The trapping times for the exponential and flat distributions are 9×10^{-13} and 2×10^{-12} s, respectively. Nevertheless, it is these small differences at short times, which contain the information on the distinguishing features of the two different distributions.

Figure 2 demonstrates, for the flat distribution, the effects of bandwidth limitation on the form of the transient decay, using time constants τ_i of 10^{-11}, 10^{-10}, and 10^{-9} s. For times $<\tau_i$, the transient is effectively being *integrated* by the responding system, and a noticeable ''overshoot'' also appears in the response, so that the observed decay does not approach the true curve until, in this case, a time of around $10\tau_i$ has elapsed. Such behavior is also often seen in the experiment, where the practice normally would be to use *only the longer time data*, for which the overshoot error is small, or to try to remeasure with a shorter response time, at the expense of reduced sensitivity.

In Fig. 3, we show the DOS computed from the full TPC and bandwidth-limited data derived from the two responses of Fig. 1, using a response time of 10^{-10} s, i.e., about 100 times longer than the respective trapping times. Arrows on Fig. 2 indicate the start point of the numerical Fourier integration, for the flat DOS TPC. The lower arrow indicates the point on the exact TPC curve, used to start the ''truncated'' case integration, while the upper arrow indicates the integration start point on the dashed curve which represents the bandwidth-limited situation. A similar procedure was carried out for the exponential DOS. It is quite clear that *truncation* of the full TPC results in loss of the short time information, resulting in computed distributions which are substantially exponential in form for both cases, and which are in error over the whole relevant energy range. Even for the case

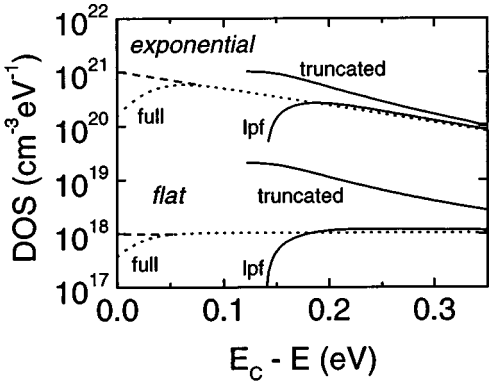

FIG. 3. Density of states computed from full TPC and truncated and bandwidth-limited TPC data of Fig. 1. *Data truncation* at 10^{-10} s results in erroneous exponential DOS. *Bandwidth limitation (lpf)* with response time 10^{-10} s results in more accurate DOS for both exponential and flat distributions. The dashed lines represent the *original* DOS at shallow energies.

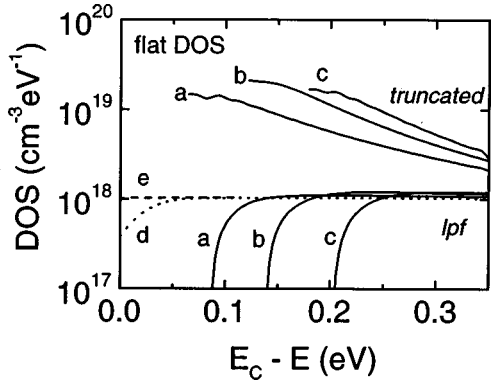

FIG. 4. Density of states computed from flat DOS TPC data of Fig. 2. Range of truncation and response times: (a) 10^{-11} s, (b) 10^{-10} s, and (c) 10^{-9} s. *Truncated data* lead to completely erroneous exponential distributions. *Bandwidth-limited (lpf)* data lead to distributions which match the DOS obtained from the full TPC (d). Also included: original DOS (e).

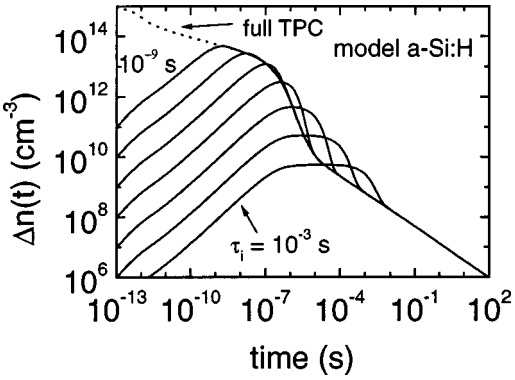

FIG. 5. Computed full TPC and bandwidth-limited TPC [in the form of electron density decay $\Delta n(t)$] for model *a*-Si:H DOS. Characteristic system times 10^{-9}–10^{-3} s. Note deep trapping at 10^{-7}–10^{-5} s. Also visible is overshoot feature associated with limited bandwidth.

where the starting distribution is exponential, the returned DOS has a significantly different characteristic slope. However, using the apparently distorted *bandwidth-limited* data results in returned distributions which agree well with the actual DOS in the energy range defined by the time response of the system.

We show in Fig. 4 the DOS returned from the TPC computed for the flat distribution, for truncation and response times of 10^{-11}, 10^{-10}, and 10^{-9} s, as illustrated in Fig. 2. The truncated data give rise to completely erroneous exponential distributions over the entire energy range employed, while the bandwidth-limited data give distributions that match the original at successively deeper energies.

From the foregoing, it is evident that the bandwidth-limited traces carry information on events which occurred at much shorter times than the bandwidth seems to allow, information which is essential to the reconstruction of the DOS. This fortuitous result relies on the integrating function of the instrumentation at short times. Splitting the Fourier transform of the TPC, Eq. (2), into short and long time portions, we have

$$I(\omega)=\int_0^{\tau_i} i(t)\exp(-j\omega t)dt+\int_{t>\tau_i}^{\infty} i(t)\exp(-j\omega t)dt. \quad (4)$$

For $\omega \gg 1/\tau_i$, the $\exp(-j\omega t)$ factor within the integrand of the first term in Eq. (4) has a very small imaginary part and is close to unity, and so can be removed from within the integral giving approximately

$$I(\omega)\approx\exp(-j\omega\tau_i)\int_0^{\tau_i} i(t)dt+\int_{t>\tau_i}^{\infty} i(t)\exp(-j\omega t)dt. \quad (5)$$

Thus if we take the numerical Fourier integral of $i(t)$ data which are accurate at time τ_i, and start the integration from time τ_i using the second term of the right hand side of Eq. (5), then this represents the truncated case described above. Although the data may be accurate over the range of the integration, nevertheless the information from shorter times, contained in the first term, is lost. However, the first integral of Eq. (5) is an operation that is performed *in reality* over this time range by the low-pass system characteristic. The bandwidth-limited response is a good approximation to this ''missing'' integral. Consequently the transform accuracy may be improved by including this response, as shown formally by the two equations. Thus, starting the numerical Fourier integral $I_n(\omega)$ at time τ_i with the *bandwidth-limited* trace, will automatically include the *system-originated* integral, thereby improving accuracy. Unfortunately, in this case, any overshoot present will also be included in the integral, producing some error, which is evident in the ''turn-down'' of the computed DOS at shallow energies in Figs. 3, 4, and 7.

B. Model amorphous silicon distribution

Figure 5 shows the full TPC computed for the model *a*-Si:H DOS given in Sec. II, and also the bandwidth-limited response calculated for characteristic system times of 10^{-9}–10^{-3} s in decade steps. The steep fall between 10^{-7} and 10^{-5} s is caused by deep trapping into the defect ''bump'' placed at 0.60 eV depth. Associated with this fall is the ''overshoot'' distortion feature described above, which is evident for system response times longer than $\sim 10^{-6}$ s, and which is also often observed in experimental TPC measurements on *a*-Si:H and related materials. It is also clear that following such an overshoot, the trace does not approach the exact TPC until around ten times the response time. Nor-

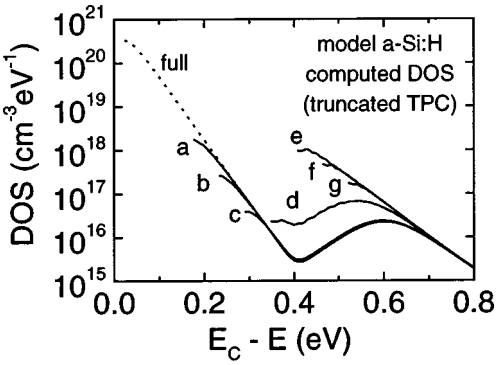

FIG. 6. Density of states for model *a*-Si:H computed from full TPC, and TPC truncated at times 10^{-9}–10^{-3} s. Truncation times of 10^{-5} s and longer lead to successively greater error in returned DOS.

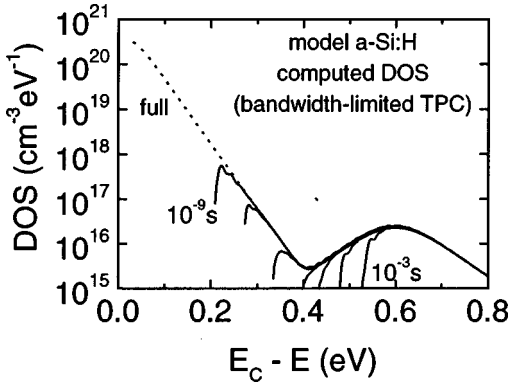

FIG. 7. Density of states for model *a*-Si:H computed from full TPC, and from apparently distorted bandwidth-limited TPC. Over the energy range for which the method is valid, the shape of the deep state DOS, is recovered accurately.

mally, only experimental data after such distortion had become negligible would be processed to compute the DOS.

In Fig. 6 we show the DOS computed from the exact TPC, simply truncated at times 10^{-9}–10^{-3} s, superimposed on the DOS obtained by using all of the TPC. The form of the ''true'' DOS can be seen to be a steep exponential tail, a deep defect bump centered at 0.60 eV, and with a minimum at ~0.4 eV. We note here that the extensive power-law decay at long times could be misinterpreted under multitrapping theory, to indicate a featureless exponential DOS. In fact, as we showed in an earlier work[10] when the short-time data before the steep fall are included, the deep defect structure in the DOS is revealed. However, for truncation times of 10^{-5} s and longer, the form of the bump is completely lost, and only an exponential distribution is returned. For a truncation time of 10^{-6} s, we begin to see that there is a deep feature, but the result is clearly substantially in error. In Fig. 7 we show the DOS computed using the apparently distorted bandwidth limited traces, processed using the procedure outlined in Sec. III A. Over the energy range for which the method is valid, it is clear that it is possible to recover the shape of the deep state DOS accurately.

Using the model DOS listed above for *a*-Si:H, it is also possible to calculate the MPC $I(\omega)$ *directly*, under bandwidth-limited conditions, by including the measuring system frequency response, prior to computing the DOS. If this is done, the results are almost identical to those of Fig. 7. Thus the question raised in Sec. I is answered—the two techniques of MPC and TPC are indeed formally equivalent *in practice*—leaving any advantage of one over the other to the properties of the instrumentation employed.

IV. CONCLUSIONS

We have examined the effects of bandwidth limitation on the accuracy of procedures used to determine the density of states from TPC and MPC data. We have highlighted the importance of missing short-time information in the TPC Fourier transform procedure, and have shown that information originating at times much shorter than the instrumentation rise time is nevertheless manifested in experimentally acquired photocurrent decay, via inclusion of the system integration of the short-time data. Using this information appropriately allows a substantial improvement in the reliability and accuracy of the determination of the DOS from TPC.

ACKNOWLEDGMENTS

The authors wish to acknowledge support from the 'Going Global' STEP collaboration program of the Association of Universities and Colleges of Canada, and EPSRC research Grant No. GR/M16696.

[1] C. Main, R. Brüggemann, D. P. Webb, and S. Reynolds, Solid State Commun. **83**, 401 (1992).
[2] J. M. Marshall, Rep. Mod. Phys. **46**, 1235 (1983).
[3] H. Naito and M. Okuda, J. Appl. Phys. **77**, 3541 (1995).
[4] H. Oheda, J. Appl. Phys. **52**, 6693 (1981).
[5] R. Brüggemann, C. Main, J. Berkin, and S. Reynolds, Philos. Mag. B **62**, 29 (1990).
[6] K. Hattori, Y. Adachi, M. Anzai, H. Okamoto, and Y. Hamakawa, J. Appl. Phys. **76**, 2841 (1994).
[7] C. Main, Mater. Res. Soc. Symp. Proc. **467**, 167 (1997).
[8] D. P. Webb, C. Main, S. Reynolds, Y. C. Chan, Y. W. Lam, and S. K. O'Leary, J. Appl. Phys. **83**, 4782 (1998).
[9] D. P. Webb, PhD thesis, University of Abertay Dundee, 1994.
[10] C. Main, R. Brüggemann, D. P. Webb, and S. Reynolds, J. Non-Cryst. Solids **165/166**, 481 (1993).
[11] S. Grabtchak, C. Main, and S. Reynolds, J. Non-Cryst. Solids **226–269,** 362 (2000).
[12] H. Michiel, J. M. Marshall, and G. J. Adriaenssens, Philos. Mag. B **48**, 187 (1983).
[13] S. Grabtchak and M. Cocivera, Phys. Rev. B **58**, 12594 (1998).
[14] C. Main, J. Berkin, and A. Merazga, in *New Physical Problems in Electronic Materials*, edited by M. Borissov, N. Kirov, J. M. Marshall, and A. Vavrek (World Scientific, Singapore, 1991), p. 55.